ECONOMIC AND ENVIRONMENTAL IMPACTS OF DIFFERENT ANTIFOULING STRATEGIES FOR FISHING BOATS IN TURKEY

Soonseok SONG[1], Claire DE MARCO MUSCAT-FENECH[2], and Yigit Kemal DEMIREL[1]

ABSTRACT

Biofouling on a ship hull increases the ship resistance and, consequently, the fuel consumption and greenhouse gas emission. Inadequate antifouling strategies may waste a significant amount of fuel and thus aggravate the profitability of the fishing boats, while resulting environmental problems. This study aims to investigate the economic and environmental impacts of different antifouling strategies with a focus on the fishing boats in Turkish fishing regions. A time-dependant biofouling growth model and the boundary layer similarity law analysis were adopted to predict the added resistance due to the fouling on the hull with different antifouling strategies. In addition, life-cycle analysis and life-cycle cost analysis were performed to estimate the economic and environmental impacts.

Keywords: Fishing Boat, Energy Efficiency, Biofouling, Life-cycle Analysis

1. Introduction

In Turkey, there are 13,000 artisanal fishing boats contributing to the income of at least 40,000 fishermen and their families constituting local communities. Often the fishing boats are of traditional design and thus inefficient in terms of fuel consumption. The fishing boats may waste up to 44% of fuel due to biofouling (organisms growing on boats), which also requires costly hull cleaning and antifouling procedures. Inadequate antifouling strategies aggravate the profitability and cause environmental problems such as increased Green-House Gas emissions and transportation of harmful non-indigenous species. Within this context, it is essential to mitigate such penalties, and the application of antifouling (AF) coatings has been the most prevalent form of mitigation. However, most of the conventional AF paints contain toxic chemicals (i.e. biocides) that may cause additional impacts persisting in the environments thereby contaminating the food chain.

Proper life-cycle assessment (LCA) and life-cycle cost analysis (LCCA) are essential to compare the pros and cons of different antifouling strategies in economic and environmental perspectives. Correspondingly, many studies have been devoted to assessing the impact of biofouling on ship performance, and many methodologies have been developed to predict the increase in the ship resistance and powering due to biofouling, using theoretical and numerical techniques (Schultz, 2007; Schultz et al., 2011; Turan et al., 2016; Demirel et al., 2017a; Demirel et al., 2017b; Farkas et al., 2018; Demirel et al., 2019; Farkas et al., 2019; Song et al., 2019; Uzun et al., 2019; Farkas et al., 2020a; Farkas et al., 2020b; Song et al., 2020a; Song et al., 2020b; Song et al., 2020c; Song et al., 2020d; Farkas et al., 2021; Song et al., 2021a; Song et al., 2021b; Song et al., 2021c). However, still not much attention has been given to the economic and environmental impacts of biofouling and antifouling strategies over the life-cycle of fishing boats.

In this study, a LCA and LCCA have been conducted to assess the environmental and economic impacts of fishing boats with different antifouling strategies. The time-dependent biofouling growth model of Uzun et al. (2019) has been adopted to predict the biofouling accumulation on 8m and 20m fishing boats operating in the Black Sea, Aegean Sea, Mediterranean Sea and Marmara Sea, Turkey with different hull cleaning frequencies. The predicted time-dependent biofouling conditions were then converted to the equivalent sand grain roughness heights to be used for predicting the added resistance through the boundary layer similarity law scaling method (Granville, 1958). Based on the resistance prediction, the fuel consumption, and CO_2 emissions of the fishing boats were predicted throughout the lifetime.

1 Department of Naval Architecture, Ocean and Marine Engineering, University of Strathclyde, 100 Montrose Street, Glasgow, UK, e-mail: soonseok.song@strath.ac.uk
2 Faculty of Engineering, University of Malta, Msida, MSD2080, Malta

2. Methodology

2.1. Time-dependent biofouling growth model

In this study, the time-dependent biofouling growth model of Uzun et al. (2019) was adopted to predict the biofouling growth on the fishing boats operating in the Black Sea, Aegean Sea, Mediterranean Sea and Marmara Sea. Uzun et al. (2019)'s biofouling growth model was developed based on 2-3 years long field data. The model reflects the three steps of biofouling accumulation (i.e. delay, growth and saturation). In the biofouling growth model, the fouling severity is expressed with the Fouling Rating (FR) values for the slime and non-shell organisms and the surface coverage (SC) of the calcareous type fouling and can be expressed by following equations.

$$FR_{Total} = FR_{Slime} + FR_{Non-shell} \tag{1}$$

$$FR_{Slime} = 20 \exp\left(-\left(\frac{t-A}{B}\right)^2\right) \tag{2}$$

$$FR_{Non-shell} = 50 \exp\left(-\left(\frac{t-C}{D}\right)^2\right) \tag{3}$$

$$SC = \frac{p}{1+\exp\left(b-ct\right)} + \frac{d}{1+\exp\left(f-gt\right)} \tag{4}$$

where, t is the immersion time of the surface in days. Uzun et al. (2019) derived the coefficients (A, B, C, D, p, b, c, d, f, g) for Self-Polishing Copolymer (SCP) type coatings from the field tests conducted at Equatorial and Mediterranean regions, respectively. Uzun et al. (2019) also suggested estimating the coefficients for other regions by linear interpolating the coefficients based on the annual average temperatures of the sea waters in different regions. Table 1 shows the coefficients in the Equatorial and Mediterranean regions of Uzun et al. (2019) and the interpolated coefficients for the Black Sea, Aegean Sea, Mediterranean Sea and Marmara Sea. The annual average values of the Sea Temperatures in the different regions were determined based on the latitude coordinates of the fishing regions as used by Uzun et al. (2019).

Table 1. Coefficients for the biofouling growth model derived by Uzun et al. (2019) and the interpolated results for the Turkish fishing reg**ions**

	Coefficients of Uzun et al. (2019)		Interpolated results		
	Equatorial region	Mediterranean Sea	Black Sea	Aegean Sea	Marmara Sea
Temp. (ºC)	27.50	16.7	14.6	16.6	15.1
A	271.400	383.5	405.2	384.0	399.9
B	73.110	124.4	134.3	124.6	131.9
C	87.000	271.9	307.8	272.8	298.9
D	37.080	99.3	111.4	99.6	108.4
p	97.000	50.0	40.9	49.8	43.1
b	16.000	32.8	36.1	32.9	35.3
c	0.041	0.047	0.048	0.047	0.048
d	3.500	0.005	-0.673	-0.011	-0.505
f	10.320	10.0	9.9	10.0	10.0
g	0.776	40.0	47.6	40.2	45.7

The FR_{Total} and SC values can be converted to the equivalent sand-grain roughness height, k_s, using the following equation from Uzun et al. (2019).

$$k_s = \begin{cases} 0.007143\, FR_{Total}^2 + 13.36\, FR_{Total} + 30 & , \quad SC < 5 \\ 2.4669\, SC^2 - 24.84 SC + 1065.7 & , \quad 5 \le SC < 50 \\ 80\, SC + 2000 & , \quad 50 \le SC \end{cases} \tag{5}$$

Figure 1 shows the calculated k_s versus the total immersion time of fishing boats in the different Turkish fishing regions.

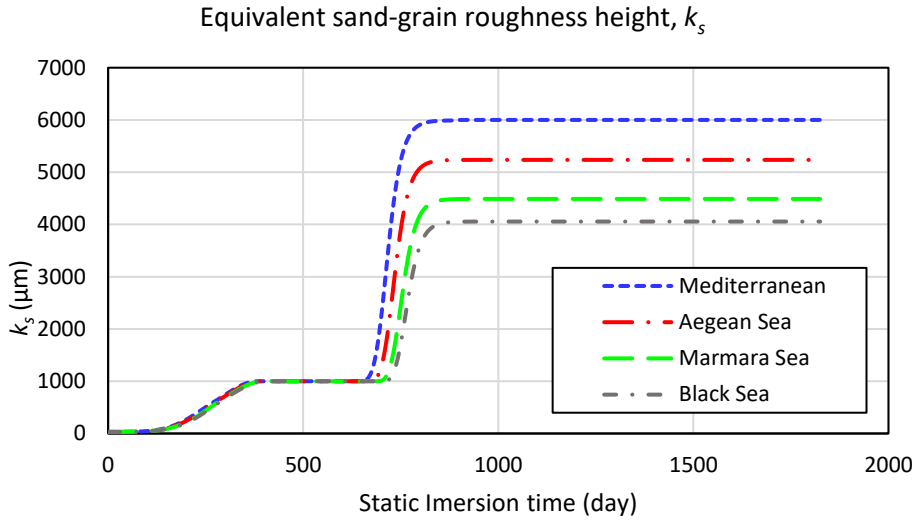

Figure 1. k_s values versus the immersion time of the fishing boats in different fishing regions

2.1. Fishing boat and operation scenarios

In this study, the LCA and LCCA were conducted based on a 8m-long and a 20m-long fishing boats operating in the Turkish fishing regions. Table 2 shows the principal particulars of the fishing boats. It is of note that the daily fuel consumption values were estimated based on the engine size, distance to the fishing ground, engine and fuel type following the method of Fisherman's workbook (FAO, 1990) without considering the fouling penalty. The fishing ban periods (i.e. off-season, 15 April – 31 August) were considered for the 20m fishing boat, while no off-season is applied to the 8m fishing boat.

Different antifouling strategies were used for the analysis including the hull-cleaning with different frequencies (i.e. 1, 2, 3 and 5 year intervals) as well as no-cleaning and hull grooming scenarios as shown in Table 2. The fouling conditions of the fishing boats over the lifetime were estimated based on the accumulative static immersion time (i.e. idle time) of the fishing boats. For the hull-cleaning scenarios, it was assumed that the hull surfaces return to unfouled surface (i.e. $FR = 0$ and $k_s = 30$) after the cleaning, while the hull fouling of the no-fouling case keeps accumulating.

Hull grooming is a proactive method that involves frequent mechanical maintenance to prevent fouling organisms from settling on the hull surface in the first place. According to Tribou and Swain (2010, 2017) groomed SCP surfaces can be maintained with no more than a very thin biofilm (coverage of < 5%). Correspondingly, the fouling condition of the groomed cases were remained to be $FR_{Slime} = 1$.

The fishing ban seasons (i.e. off-seasons) were applied to the 20m fishing boats, while no restriction is applied to the 8m fishing boats, and it was assumed that the fishing boats were kept dry during the off-seasons and the hull fouling stops growing.

Table 2. Principal particulars and the operational conditions of the fishing boats

	8m fishing boat	20m fishing boat
Length	8m	20m
Engine Power	31 HP	550 HP
Fuel type	Diesel	Diesel
Speed	6 knots	9 knots
Distance to fishing ground	20 Nautical mile	20 Nautical mile
Daily fuel consumption	37 L	200 L
Fishing ban season	N/A	15 April – 31 August (every year)
Operation condition	6 days week	6 days week
Antifouling strategies	Grooming 1-year cleaning 2-year cleaning 3-year cleaning 5-year cleaning No cleaning	Grooming 1-year cleaning 2-year cleaning 3-year cleaning 5-year cleaning No cleaning

3. Results

Figures 2 and 3 show the k_s values on the 8m and 20m fishing boats in different fishing regions with different hull cleaning methods. Due to the similar annual sea temperatures of Mediterranean Sea and Aegean Sea, the k_s growths of the fishing boats in these regions show similar values. It is notable that the k_s values of the 8m fishing boat are higher than those of the 20m fishing boat, and it can be attributed to the fishing-ban seasons (i.e. off-seasons) that were applied only on the 20m fishing boat. Due to this difference, the 3-year hull cleaning scenarios of the 8m fishing boats reached to high k_s values.

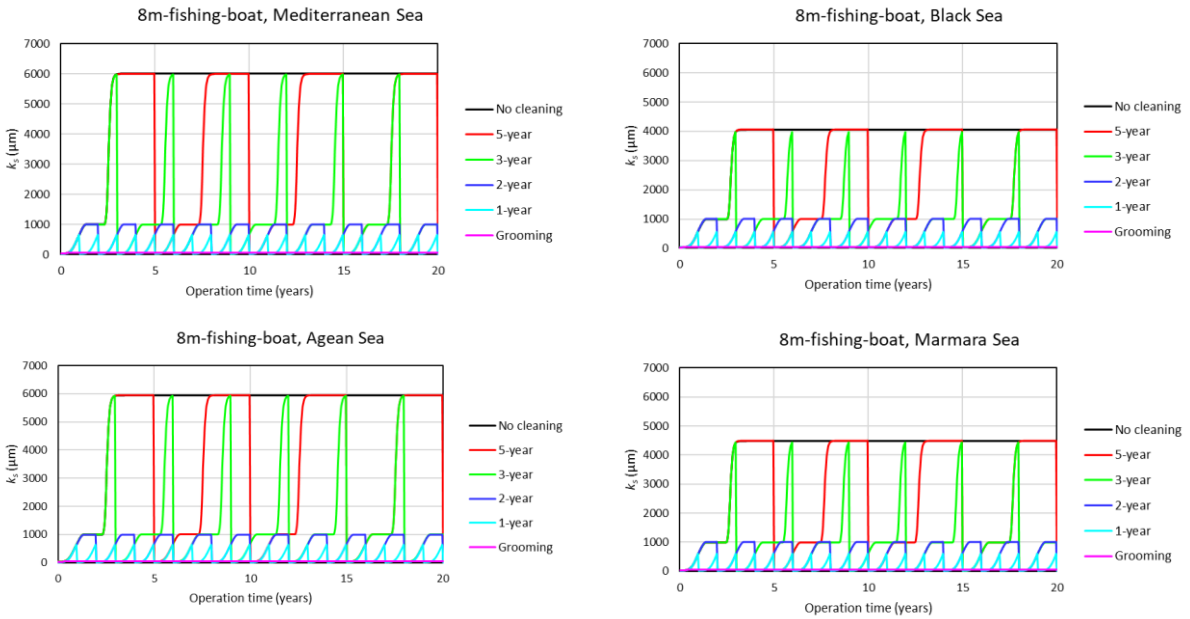

Figure 2. Equivalent sand-grain roughness height, k_s of the 8m fishing boats with different hull cleaning intervals in the Turkish fishing regions

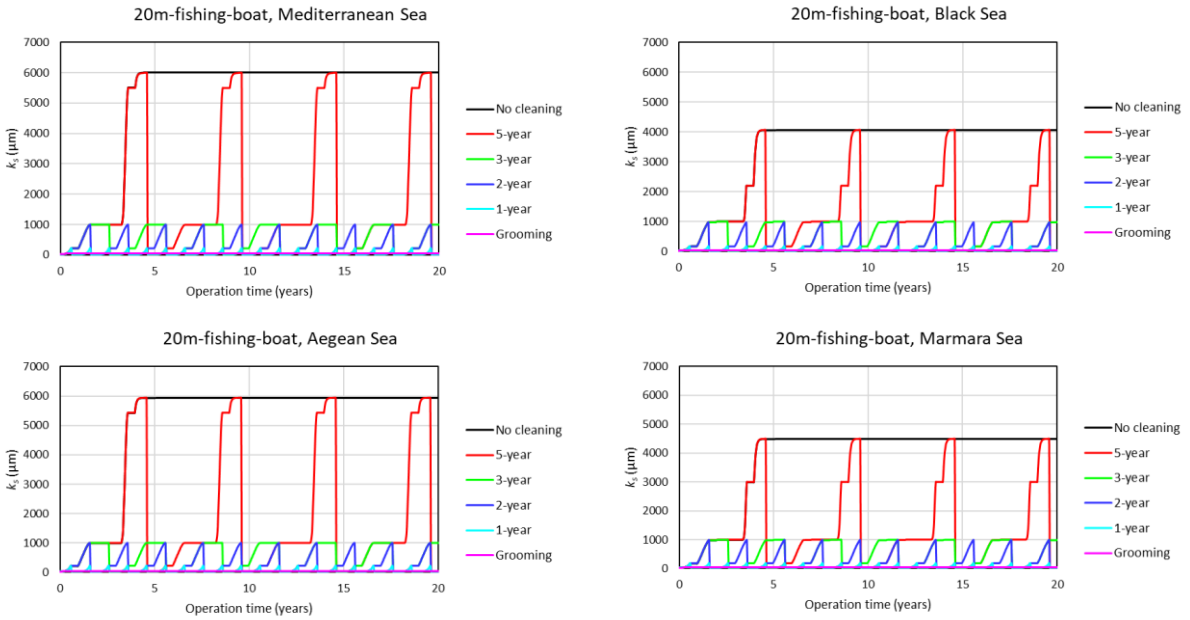

Figure 3. Equivalent sand-grain roughness height, k_s of the 20m fishing boats with different hull cleaning intervals in the Turkish fishing regions

Using the obtained k_s values over time, the added resistance of the fishing boats were predicted following the similarity law scaling procedure proposed by Granville (1958). The total resistance, R_T, of the fishing boats was estimated using the obtained added resistance and the residuary resistance of a fishing boat obtained by Ali et al. (2019). The percentage increase in the effective power, $\%\Delta P_E$, of the fishing boats was calculated as,

$$\%\Delta P_E = \frac{P_{E_{fouled}} - P_{E_{clean}}}{P_{E_{clean}}} \times 100\% \quad (6)$$

$$= \frac{V_{ship} R_{T_{fouled}} - V_{ship} R_{T_{clean}}}{V_{ship} R_{T_{clean}}} \times 100\%$$

$$= \frac{R_{T_{fouled}} - R_{T_{clean}}}{R_{T_{clean}}} \times 100\%$$

Figure 4 and 5 show the $\%\Delta P_E$ values of the 8m and 20m fishing boats in different fishing regions with different hull cleaning methods. The results show that the $\%\Delta P_E$ values of the 8m fishing boat in Mediterranean and Aegean Seas can increase by 53%, 53%, 53%, 24%, 19%, and 0.3% with the antifouling strategies of no-cleaning, 5-year, 3-year, 2-year, and 1-year interval cleanings and hull grooming, respectively. For the same antifouling strategies, the $\%\Delta P_E$ values of the 8m fishing boat increase up to 45%, 45%, 45%, 24%, 18%, and 0.3% in the Black Sea and 47%, 47%, 47%, 24%, 16%, and 0.3% in the Marmara Sea, respectively.

On the other hand, the $\%\Delta P_E$ values of the 20m fishing boat in the Mediterranean and Aegean Seas showed increases up to 48%, 48%, 23%, 23%, 11%, and 0.7% with the antifouling strategies of no-cleaning, 5-year, 3-year, 2-year, and 1-year interval cleanings and hull grooming, respectively. For the same antifouling strategies, the $\%\Delta P_E$ values of the 20m fishing boat increase up to 41%, 41%, 23%, 23%, 8%, and 0.7% in the Black Sea and 43%, 43%, 23%, 23%, 9%, and 0.7% in the Marmara Sea, respectively.

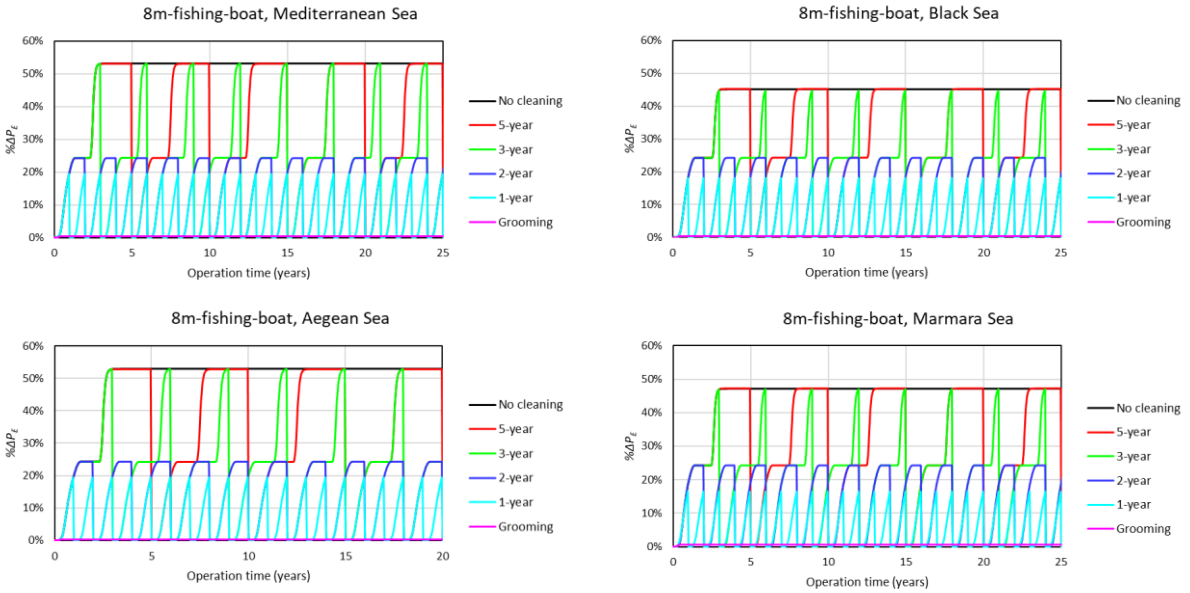

Figure 4. % increase in effective power, $\%\Delta P_E$ of the 8m fishing boats with different hull cleaning intervals in the Turkish fishing regions

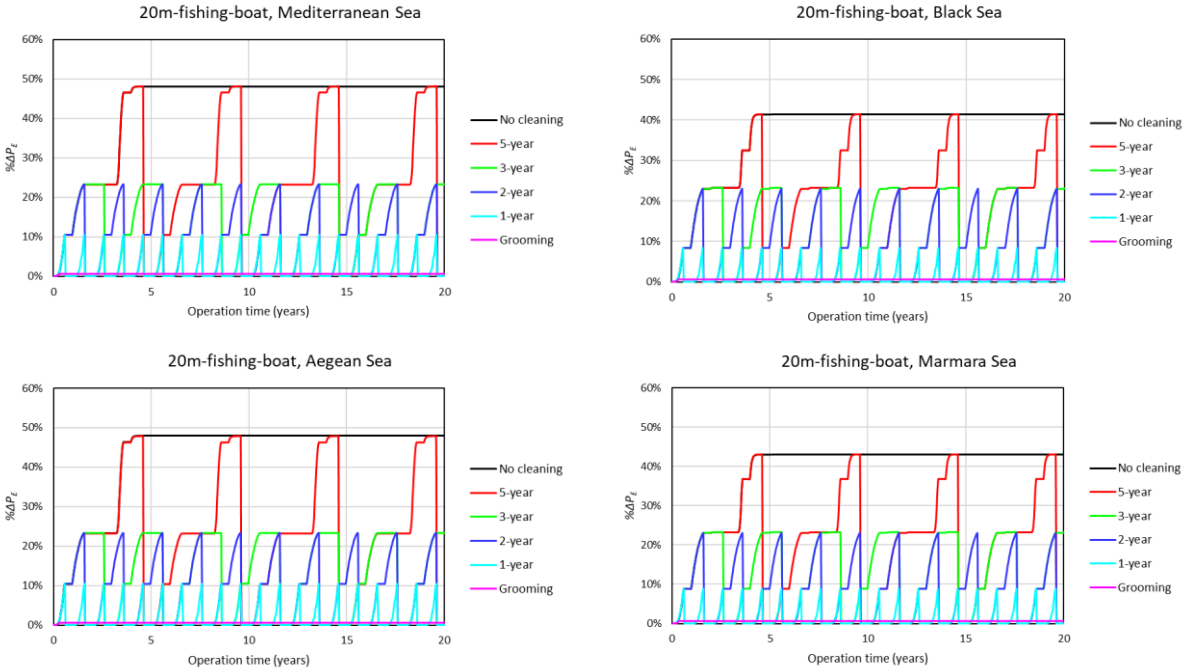

Figure 5. % increase in effective power, $\%\Delta P_E$ of the 20m fishing boats with different hull cleaning intervals in the Turkish fishing regions

The fuel consumptions of the fishing boats with different antifouling strategies were predicted based on the assumption that the daily fuel consumption of the fishing boats is proportional to the effective power P_E of the fishing boat. Using the daily fuel consumption of the fishing boats without the hull fouling (Table 2) and the $\%\Delta P_E$ values, the fuel consumptions of the fishing boats with different antifouling strategies were estimated.

Figures 6 and 7 show the cumulative fuel consumptions of the 8m and 20m fishing boats in the Turkish fishing regions with different antifouling strategies. The data predicted that the 8m fishing boat consumes a total of 343,000L, 329,000L, 344,000L, and 331,000L over the 20-year operational period if the no cleaning strategy is used in the Mediterranean, Black, Aegean, and Marmara Seas, respectively; whilst if a hull grooming strategy is adopted the fuel consumption can be reduced to 233,000L, 232,000L, 230,000L, and 233,000L respectively.

With a no cleaning strategy the 20-year fuel consumption for the 20m fishing boats were predicted to be 2,406,000L, 2,308,000L, 2,403,000L and 2,332,000L in the Mediterranean, Black, Aegean, and Marmara Seas, respectively, and can be reduced to 1,714,000L, 1,708,000L, 1,702,000L and 1,719,000L when the hull grooming strategy is adopted.

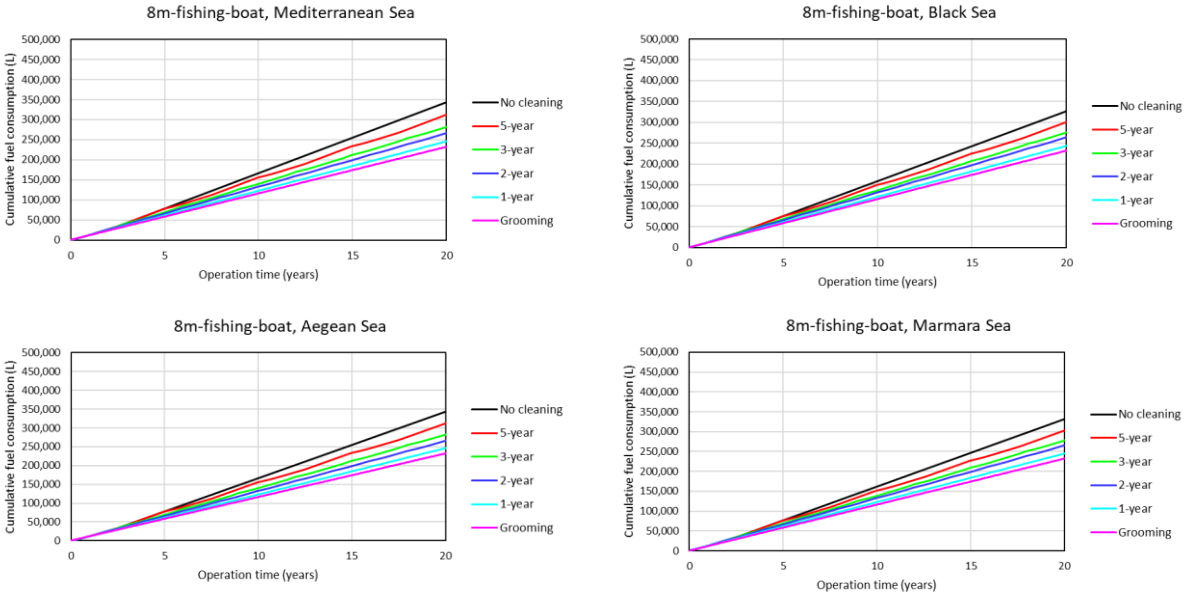

Figure 6. Cumulative fuel consumptions of the 8m fishing boats with different hull cleaning intervals in the Turkish fishing regions

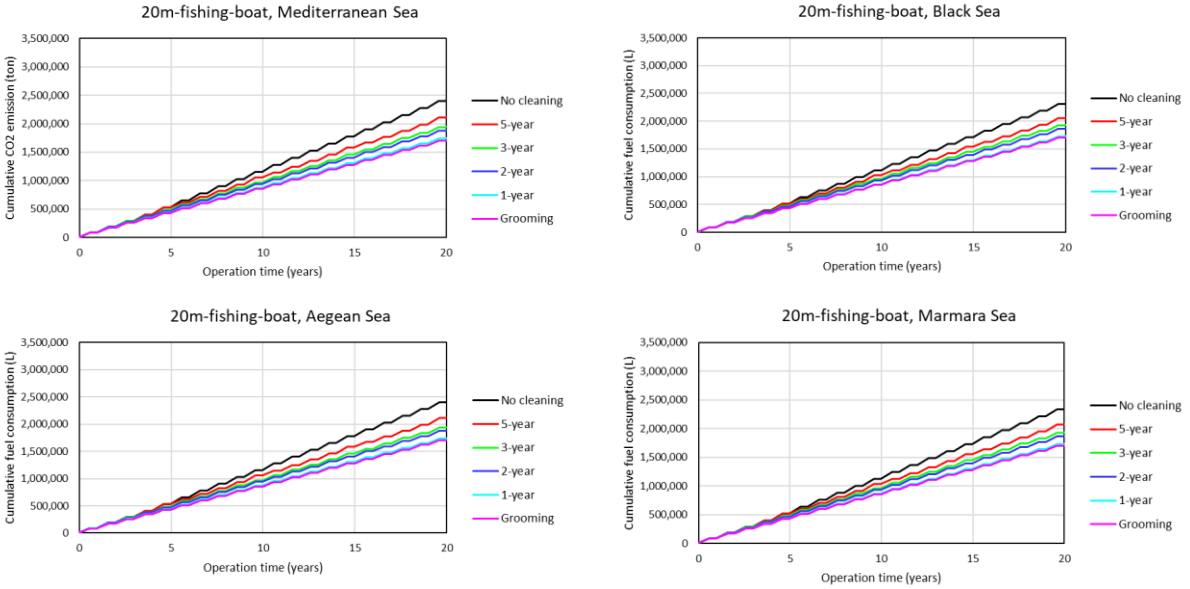

Figure 7. Cumulative fuel consumptions of the 20m fishing boats with different hull cleaning intervals in the Turkish fishing regions

Using the fuel consumption predictions, the fuel costs were evaluated based on the average fuel price of red diesel in 2019 (£ 0.6275 per L) provided in https://ahdb.org.uk/fuel-prices. Figures 8 and 9 compare the total fuel costs of the 8m and 20m fishing boats spent during the 20-year operational times.

The data predicts that the 8m fishing boat with the no cleaning strategy will spend £215,839, £205,451, £215,548 and £207,986 in the Mediterranean, Black, Aegean, and Marmara Seas, respectively over the 20-year operations, and can be reduced to £145,767-8 with the hull grooming strategy. In terms of the 20m fishing boats with the no cleaning strategy, total fuel costs of £1,514,469, £1,452,891, £1,512,850, and £1,468,005 were expected in the Mediterranean,

Black, Aegean, and Marmara Seas, respectively during the 20-year operations, while these can be reduced to £1,071,527 with the hull grooming strategy.

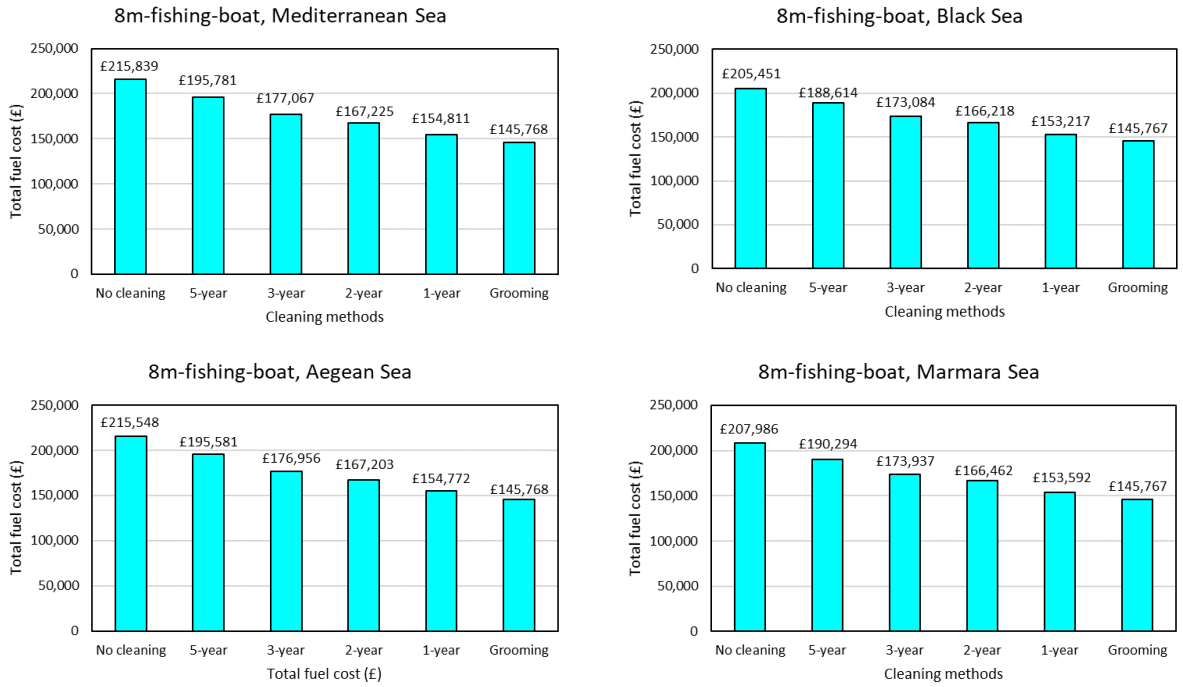

Figure 8. Total fuel costs of the 8m fishing boats with different hull cleaning intervals in the Turkish fishing regions

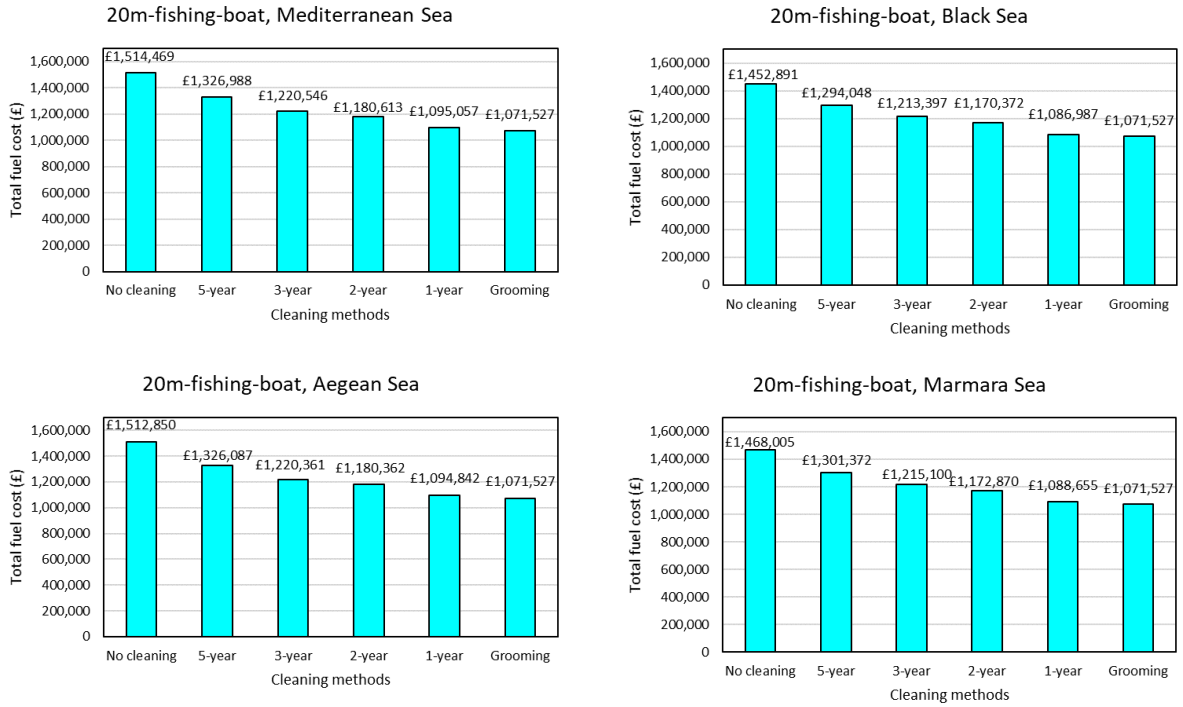

Figure 9. Total fuel costs of the 20m fishing boats with different hull cleaning intervals in the Turkish fishing regions

The carbon dioxide (CO_2) emissions of the fishing vessels were estimated using the fuel consumption predictions with different antifouling strategies. Red diesel is known to emit 2.9 kg of CO_2 per litre, and therefore, the fuel consumptions can be converted CO_2 emissions into the air from the fishing vessels.

The data predicts that, under the no cleaning scenario, the 8m fishing boat will emit 1,164, 1,108, 1,162, and 1,121 metric ton of CO_2 into the air during the 20-year operation times in the Mediterranean, Black, Aegean, and Marmara Seas, respectively. The emissions can be reduced to 786 metric ton if the hull grooming strategy is used. On the other hand, the CO_2 emissions of the 20m fishing boat over the 20-year operations were predicted to be 8,166, 7,834, 8,157, and 7,915 metric ton with the no cleaning strategy, while these can be reduced to 5,777 metric ton if the hull grooming strategy is used.

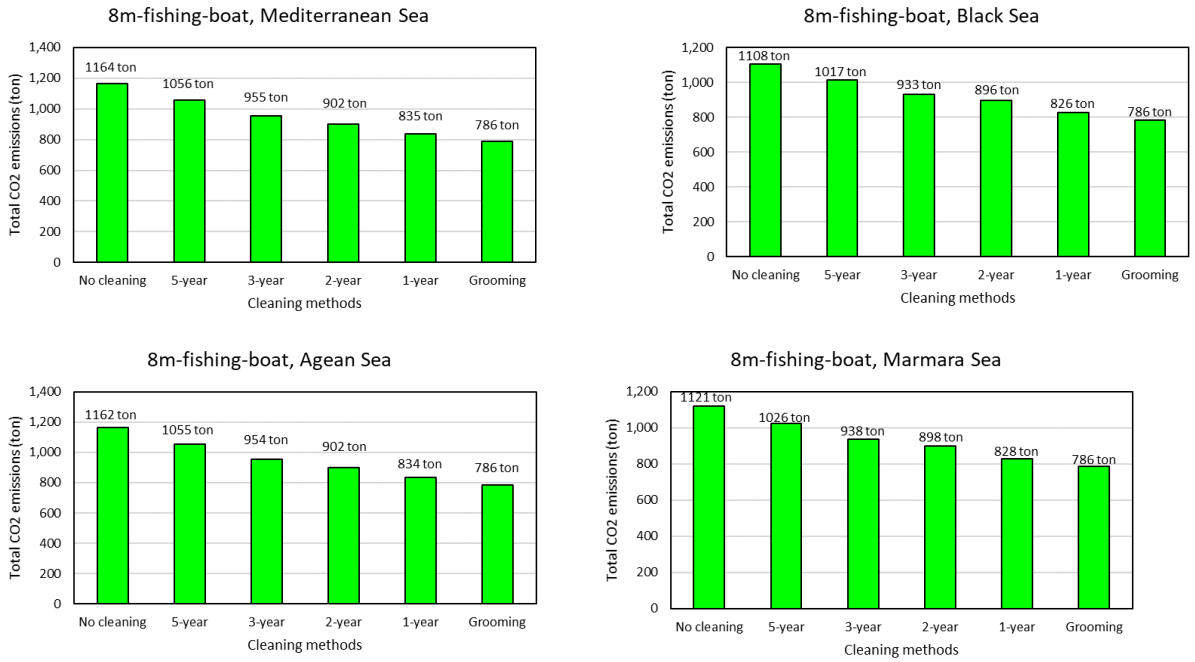

Figure 10. Total CO_2 emissions of the 8m fishing boats with different hull cleaning intervals in the Turkish fishing regions

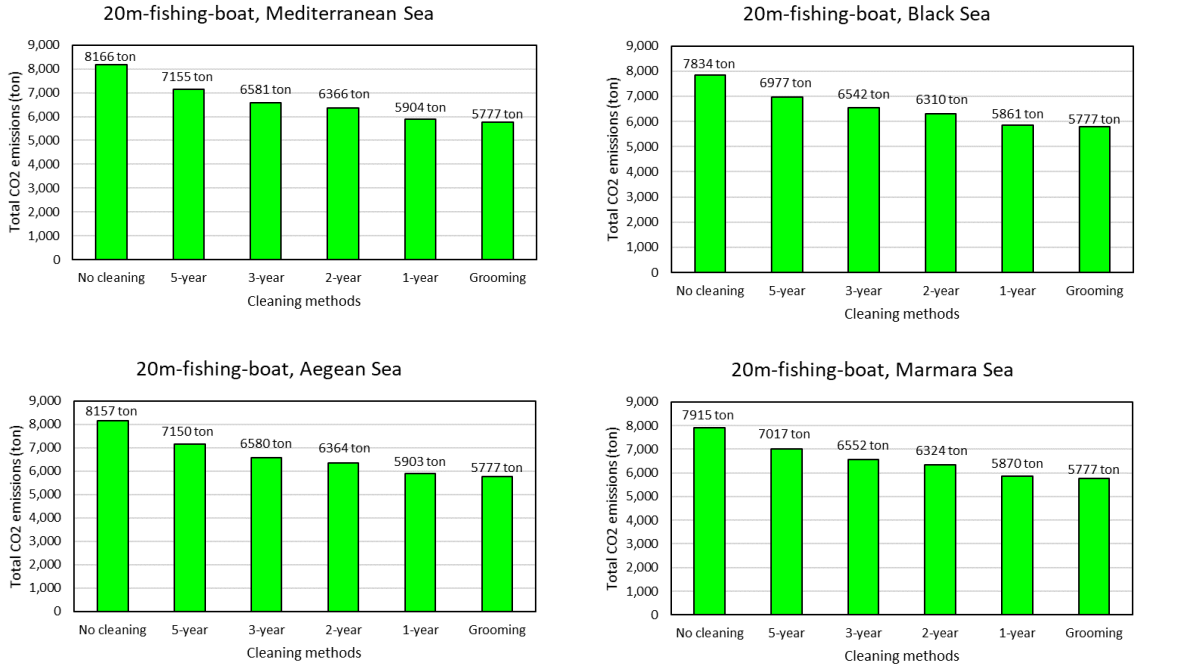

Figure 11. Total CO_2 emissions of the 20m fishing boats with different hull cleaning intervals in the Turkish fishing regions

4. Concluding remarks

In this study, the economic and environmental impacts of different antifouling strategies were described. A time-dependent biofouling growth model was adopted to predict the biofouling growth on 8m and 20m fishing boats in different Turkish fishing regions (i.e. Mediterranean Sea, Black Sea, Aegean Sea and Marmara Sea) over a 20-year operational life-time, with different antifouling strategies (i.e. no cleaning, 5-year cleaning, 3-year cleaning, 2-year cleaning, 1-year cleaning and hull grooming). The predicted biofouling growth was used to predict the added resistance and increase in the effective power at the same operation speed, based on the similarity law scaling method. Based on the effective power predictions, the fuel consumptions, fuel costs and CO_2 emissions were estimated for the fishing boats with different antifouling strategies in the Turkish fishing regions.

The study presented here demonstrated the feasibility of the time-dependant biofouling growth model and the similarity law scaling for the life-cycle analysis (LCA) and life-cycle cost analysis (LCCA) of fishing boats in Turkish fishing regions. The result showed that the hull-grooming strategy shows better economic and environmental performances compared to the conventional hull cleaning strategies. However, the analyses were conducted with several assumptions for simplification and the results can also differ with different fouling growth prediction models. Therefore, full-scale validation studies are encouraged to confirm the accuracy of the proposed methodology.

5. Acknowledgement

The authors are grateful for Scottish Funding Council's support for the project, *Development of smart antifouling strategies towards energy-efficient fishing boats in Turkey*.

The authors acknowledge that the research presented in this paper was carried out as part of the European Union Horizon 2020 project, *VENTuRE* (grant no. 856887).

6. References

Ali, M. A., Peng, H., & Qiu, W. (2019). Resistance prediction of two fishing vessel models based on RANS solutions. *Physics and Chemistry of the Earth, Parts A/B/C, 113*, 115-122. doi:https://doi.org/10.1016/j.pce.2019.05.005

Demirel, Y. K., Song, S., Turan, O., & Incecik, A. (2019). Practical added resistance diagrams to predict fouling impact on ship performance. *Ocean Engineering, 186*, 106112. doi:https://doi.org/10.1016/j.oceaneng.2019.106112

Demirel, Y. K., Turan, O., & Incecik, A. (2017a). Predicting the effect of biofouling on ship resistance using CFD. *Applied Ocean Research, 62*, 100-118. doi:https://doi.org/10.1016/j.apor.2016.12.003

Demirel, Y. K., Uzun, D., Zhang, Y., Fang, H.-C., Day, A. H., & Turan, O. (2017b). Effect of barnacle fouling on ship resistance and powering. *Biofouling, 33*(10), 819-834. doi:10.1080/08927014.2017.1373279

FAO. (1990). *Fisherman's workbook*. IFREMER, Sete, France: Fishery Industries Division, FAO.

Farkas, A., Degiuli, N., & Martić, I. (2018). Towards the prediction of the effect of biofilm on the ship resistance using CFD. *Ocean Engineering, 167*, 169-186. doi:https://doi.org/10.1016/j.oceaneng.2018.08.055

Farkas, A., Degiuli, N., & Martić, I. (2019). Impact of biofilm on the resistance characteristics and nominal wake. *Proceedings of the Institution of Mechanical Engineers, Part M: Journal of Engineering for the Maritime Environment*, 1475090219862897. doi:10.1177/1475090219862897

Farkas, A., Degiuli, N., & Martić, I. (2020a). An investigation into the effect of hard fouling on the ship resistance using CFD. *Applied Ocean Research, 100*, 102205. doi:https://doi.org/10.1016/j.apor.2020.102205

Farkas, A., Degiuli, N., & Martić, I. (2021). The impact of biofouling on the propeller performance. *Ocean Engineering, 219*, 108376. doi:https://doi.org/10.1016/j.oceaneng.2020.108376

Farkas, A., Song, S., Degiuli, N., Martić, I., & Demirel, Y. K. (2020b). Impact of biofilm on the ship propulsion characteristics and the speed reduction. *Ocean Engineering, 199*, 107033. doi:https://doi.org/10.1016/j.oceaneng.2020.107033

Granville, P. S. (1958). The frictional resistance and turbulent boundary layer of rough surfaces. *J. Ship Res., 2*(3), 52-74.

Schultz, M. P. (2007). Effects of coating roughness and biofouling on ship resistance and powering. *Biofouling, 23*(5), 331-341. doi:10.1080/08927010701461974

Schultz, M. P., Bendick, J. A., Holm, E. R., & Hertel, W. M. (2011). Economic impact of biofouling on a naval surface ship. *Biofouling, 27*(1), 87-98. doi:10.1080/08927014.2010.542809

Song, S., Dai, S., Demirel, Y. K., Atlar, M., Day, S., & Turan, O. (2021a). Experimental and Theoretical Study of the Effect of Hull Roughness on Ship Resistance. *Journal of Ship Research, 65*(01), 62-71. doi:10.5957/JOSR.07190040

Song, S., Demirel, Y. K., & Atlar, M. (2019). *An Investigation Into the Effect of Biofouling on Full-Scale Propeller Performance Using CFD*. Paper presented at the ASME 2019 38th International Conference on Ocean, Offshore and Arctic Engineering, Glasgow, UK. https://doi.org/10.1115/OMAE2019-95315

Song, S., Demirel, Y. K., & Atlar, M. (2020a). Propeller Performance Penalty of Biofouling: Computational Fluid Dynamics Prediction. *Journal of Offshore Mechanics and Arctic Engineering, 142*(6). doi:10.1115/1.4047201

Song, S., Demirel, Y. K., Atlar, M., Dai, S., Day, S., & Turan, O. (2020b). Validation of the CFD approach for modelling roughness effect on ship resistance. *Ocean Engineering, 200*, 107029. doi:https://doi.org/10.1016/j.oceaneng.2020.107029

Song, S., Demirel, Y. K., Atlar, M., & Shi, W. (2020c). Prediction of the fouling penalty on the tidal turbine performance and development of its mitigation measures. *Applied Energy, 276*, 115498. doi:https://doi.org/10.1016/j.apenergy.2020.115498

Song, S., Demirel, Y. K., De Marco Muscat-Fenech, C., Tezdogan, T., & Atlar, M. (2020d). Fouling effect on the resistance of different ship types. *Ocean Engineering, 216*, 107736. doi:https://doi.org/10.1016/j.oceaneng.2020.107736

Song, S., Demirel, Y. K., Muscat-Fenech, C. D. M., Sant, T., Villa, D., Tezdogan, T., & Incecik, A. (2021b). Investigating the Effect of Heterogeneous Hull Roughness on Ship Resistance Using CFD. *Journal of Marine Science and Engineering, 9*(2), 202.

Song, S., Ravenna, R., Dai, S., DeMarco Muscat-Fenech, C., Tani, G., Demirel, Y. K., Atlar, M., Day, S., & Incecik, A. (2021c). Experimental investigation on the effect of heterogeneous hull roughness on ship resistance. *Ocean Engineering, 223*, 108590. doi:https://doi.org/10.1016/j.oceaneng.2021.108590

Tribou, M., & Swain, G. (2010). The use of proactive in-water grooming to improve the performance of ship hull antifouling coatings. *Biofouling, 26*(1), 47-56. doi:10.1080/08927010903290973

Tribou, M., & Swain, G. (2017). The effects of grooming on a copper ablative coating: a six year study. *Biofouling, 33*(6), 494-504. doi:10.1080/08927014.2017.1328596

Turan, O., Demirel, Y. K., Day, S., & Tezdogan, T. (2016). Experimental Determination of Added Hydrodynamic Resistance Caused by Marine Biofouling on Ships. *Transportation Research Procedia, 14*, 1649-1658. doi:https://doi.org/10.1016/j.trpro.2016.05.130

Uzun, D., Demirel, Y. K., Coraddu, A., & Turan, O. (2019). Time-dependent biofouling growth model for predicting the effects of biofouling on ship resistance and powering. *Ocean Engineering, 191*, 106432. doi:https://doi.org/10.1016/j.oceaneng.2019.106432